



Microbial Community Structure Affects Marine Dissolved Organic Matter Composition

Elizabeth B. Kujawinski^{1*}, Krista Longnecker¹, Katie L. Barott^{1†}, Ralf J. M. Weber² and Melissa C. Kido Soule¹

¹ Department of Marine Chemistry and Geochemistry, Woods Hole Oceanographic Institution, Woods Hole, MA, USA,

² School of Biosciences, University of Birmingham, Birmingham, UK

OPEN ACCESS

Edited by:

Michael William Lomas,
Bigelow Laboratory for Ocean
Sciences, USA

Reviewed by:

Gordon T. Taylor,
Stony Brook University, USA
Jason Michel Smith,
Monterey Bay Aquarium Research
Institute, USA

*Correspondence:

Elizabeth B. Kujawinski
ekujawinski@whoi.edu

†Present Address:

Katie L. Barott,
Hawaii Institute of Marine Biology,
University of Hawaii - Manoa,
Kaneohe, HI, USA

Specialty section:

This article was submitted to
Marine Biogeochemistry,
a section of the journal
Frontiers in Marine Science

Received: 01 December 2015

Accepted: 21 March 2016

Published: 05 April 2016

Citation:

Kujawinski EB, Longnecker K,
Barott KL, Weber RJM and Kido
Soule MC (2016) Microbial
Community Structure Affects Marine
Dissolved Organic Matter
Composition. *Front. Mar. Sci.* 3:45.
doi: 10.3389/fmars.2016.00045

Marine microbes are critical players in the global carbon cycle, affecting both the reduction of inorganic carbon and the remineralization of reduced organic compounds back to carbon dioxide. Members of microbial consortia all depend on marine dissolved organic matter (DOM) and in turn, affect the molecules present in this heterogeneous pool. Our understanding of DOM produced by marine microbes is biased toward single species laboratory cultures or simplified field incubations, which exclude large phototrophs and protozoan grazers. Here we explore the interdependence of DOM composition and bacterial diversity in two mixed microbial consortia from coastal seawater: a whole water community and a <1.0- μm community dominated by heterotrophic bacteria. Each consortium was incubated with isotopically-labeled glucose for 9 days. Using stable-isotope probing techniques and electrospray ionization Fourier-transform ion cyclotron resonance mass spectrometry, we show that the presence of organisms larger than 1.0- μm is the dominant factor affecting bacterial diversity and low-molecular-weight (<1000 Da) DOM composition during this experiment. In the <1.0- μm community, DOM composition was dominated by compounds with lipid and peptide character at all time points, confirmed by fragmentation spectra with peptide-containing neutral losses. In contrast, DOM composition in the whole water community was nearly identical to that in the initial coastal seawater. These differences in DOM composition persisted throughout the experiment despite shifts in bacterial diversity, underscoring an unappreciated role for larger microorganisms in constraining DOM composition in the marine environment.

Keywords: DOM, bacteria, protozoa, microbial ecology, peptides

INTRODUCTION

Dissolved organic carbon in the oceans constitutes a significant global reservoir of carbon, comparable to atmospheric carbon dioxide (700 GT; Hedges, 2002), and its cycling affects the flux of carbon between the oceans and the atmosphere. Consequently, the production of dissolved organic matter (DOM), its residence time in the surface ocean, and its eventual remineralization to carbon dioxide, are of paramount importance in constraining the ocean-atmosphere carbon flux over long time periods. DOM is produced, in large part, by photosynthetic microbes in the surface ocean and is altered and/or remineralized by a consortium of archaea, bacteria, protozoa, viruses, and

phytoplankton, collectively known as the microbial loop (Azam et al., 1983). Metabolic capabilities within microbial consortia are determined to some extent by DOM characteristics (Baña et al., 2014), and DOM composition is affected by the individual metabolic reactions catalyzed by microbes (Alonso-Sáez et al., 2012). These microbe-DOM interactions are therefore relevant to the global carbon cycle and crucial to modeling the flow of carbon through the dissolved pool.

DOM molecules occur along a spectrum of reactivity, from labile with residence times of hours to days, to refractory with residence times from tens to thousands of years. Marine bacteria have been implicated as a large source of both labile (Kawasaki and Benner, 2006) and refractory (Ogawa et al., 2001) DOM in laboratory and field incubations. The presence of long-lived material in these incubations has been interpreted as evidence of a bacterial source of the same refractory material present in the oceans. The role of bacteria in refractory DOM production has been highlighted in the concept of the “microbial carbon pump” (Jiao et al., 2010), where bacterial refractory DOM is trapped in the deep ocean and the associated carbon is effectively sequestered from the atmosphere. Bulk compositional analysis supports this contention (e.g., presence of bacterial-derived D-amino acids in deep ocean DOM; Kaiser and Benner, 2008) although recent molecular-level investigations suggest that bacterial-derived refractory material differs structurally from refractory organic matter in the oceans (Osterholz et al., 2015). In these studies, bacteria likely dominated the incubations due to dilution, filtration or removal of light. Consequently the impact of other microbes on DOM composition may have been underestimated, particularly phytoplankton who provide bacterial growth substrates (Amin et al., 2012) and grazers who prey on bacteria (Sherr and Sherr, 1994).

Phytoplankton production of DOM is a well-known source of growth substrates for marine bacteria. Phytoplankton exudates contain monomers such as sugars and amino acids (Sarmiento et al., 2013) and complex polymers such as polysaccharides and peptides (reviewed by Carlson, 2002), as well as numerous unknown molecules (Becker et al., 2014; Longnecker et al., 2015b). Interestingly, the composition of these exudates is affected by the presence of other phytoplankton (Paul et al., 2009) or other bacteria (Durham et al., 2015). In some cases, specific interactions between phytoplankton and bacteria could be mediated through the DOM pool (Sher et al., 2011). Thus, interactions such as those between phytoplankton and bacteria, or between predatory protozoa and bacterial prey, structure microbial communities, and most likely affect DOM composition in the global ocean (Lima-Mendez et al., 2015).

Protozoa feed on bacteria, phytoplankton, and small detrital particles (Sherr and Sherr, 1994) and, in so doing, affect prey diversity, concentration, and metabolic function (Pernthaler, 2005; Alonso-Sáez et al., 2009). Through their fairly broad prey range, protozoa can respond quickly to a substrate-driven increase in prey populations (Pernthaler, 2005) and can affect the metabolic functions resident within the prey community by affecting prey diversity (Corno and Jürgens, 2008). By releasing nutrients and organic substrates (Andersson et al., 1985; Taylor et al., 1985), they stimulate the bacterial community to grow

exponentially and/or to enhance their metabolic activity (Wang et al., 2009). During grazing, protozoa have a direct impact on bacterial biomass through feeding and an indirect impact on DOM composition through release of bacterial metabolites as a dissolved waste product (Taylor et al., 1985; Fouilland et al., 2014). Protozoa typically release 10–30% of ingested carbon as DOM, including dissolved amino acids and colloidal micelles of prey organic matter (reviewed by Nagata, 2000). An important facet of this release is that it is predicated on encounter rates and ecosystem parameters, rather than on metabolic capabilities encoded in the genome of either the predator or the prey. Thus, empirical studies are needed to determine the impact of protozoan grazing on the molecular-level composition of DOM released during feeding.

Here, we examine DOM composition and cycling in two mixed microbial consortia, akin to that ubiquitously present in coastal waters. In particular, we investigated the impact of removal of large (>1.0- μm) organisms on both bacterial diversity and molecular-level DOM composition. We established parallel seawater treatments with whole water consortia or with 1.0 μm -filtered water (hereafter referred to as <1.0- μm), with additions of isotopically-labeled glucose. We used molecular biology techniques to explore microbial diversity and ultrahigh resolution mass spectrometry to assess DOM composition and to characterize the structure of selected compounds.

METHODS

Experimental Setup

Surface seawater was collected on an incoming tide from Vineyard Sound, MA (hereafter: VSW) at the WHOI dock in April 2007 ($T = 6^\circ\text{C}$). The water was transported back to the laboratory in polycarbonate carboys and half (~16L) was immediately filtered through a 1.0- μm bell filter (Whatman). The bell-filter was cleaned extensively with acidified and then neutral Milli-Q water prior to use. Sixteen parallel bottle incubations were established with 2 L each of either unfiltered VSW (“whole water”) or 1.0 μm -filtered VSW (“<1.0- μm ”). Sterile control incubations were established with 0.2- μm -filtered VSW but were contaminated after 4–5 days and were not considered further. Each incubation bottle was amended with uniformly-labeled ^{13}C -glucose (final added concentration: 1 μM) and ammonium (NH_4^+ , final added concentration: 1 μM). The glucose amendment represents an ~5% increase in dissolved organic carbon over typical VSW concentrations while the ammonium amendment is 2–3X typical VSW concentrations. These bottles were placed within a temperature-controlled incubator at 15°C on a 12 h:12 h light: dark cycle for a total of 9 days. On days 1, 2, 5, and 9, two replicate bottles from each treatment were sacrificed for microbial diversity and DOM composition analyses. Initial seawater conditions were assessed for unfiltered VSW only. The impact of 1.0- μm filtration on DOM composition was examined with follow-up tests described below. Cells were captured on combusted 0.2 μm Anodisc filters (Whatman; combusted at 400°C for at least 4 h) and DOM was extracted from the resulting filtrate.

All reagents were Optima grade or better (Fisher Scientific). All glassware was combusted at 450°C for at least 4 h. All plasticware was soaked in 10% HCl (trace-metal grade) for 12–24 h, rinsed with Milli-Q water, and autoclaved prior to use.

Dissolved Organic Matter Analyses

Samples were collected for total and dissolved organic carbon (T/DOC) and for isotopic analysis of bulk organic carbon. However, these samples were lost due to analytical error during the isotopic analysis and thus are not available for comparison with the molecular-level analyses. Consequently, we focused our results and discussion on comparing DOM composition, rather than on estimating quantitative changes in specific compound classes over the experiment.

The 0.2- μm filtrate (~ 2 L) at each timepoint was collected in 2.5-L polycarbonate bottles, acidified to pH 3 with concentrated HCl and stored in the dark at 4°C until extraction. Solid-phase extraction disks (47 mm C₁₈/SDB resin; 3M) were placed on combusted or solvent-rinsed glass frits, and pre-conditioned with acetone, methylene chloride, methanol and Milli-Q water, according to manufacturer's instructions. Without letting the disks become dry, sample was pulled through the disks by vacuum. After the entire sample went through a disk, each disk was rinsed with pH 3 Milli-Q water and allowed to dry for at least 15 min. DOM was eluted with 70% methanol. Extracts were blown down to near dryness, resuspended in a known volume of 70% methanol and stored in the refrigerator or freezer until analysis.

Due to excessive salt content, samples were purified using ZipTips (C18-embedded pipet tips; Millipore). Extracts were dried and then re-dissolved in an equivalent volume of 5% methanol and 95% Milli-Q water, adjusted to pH 3 with concentrated HCl. Ten 10- μL aliquots of sample were extracted onto the C18 resin in the ZipTip. The sample was washed with five 10- μL aliquots of pH 3 Milli-Q water and eluted with two 5- μL aliquots of methanol. The volume was adjusted to 100 μL with 70% methanol. Purification efficiencies could not be calculated for this process given the small sample volumes. However, all samples were treated identically.

All extracts were analyzed in positive ion mode at the WHOI FT-MS facility on a 7T hybrid linear ion-trap Fourier transform ion cyclotron resonance mass spectrometer (LTQ-FT-ICR MS, Thermo Scientific, Waltham MA). Samples were amended with 0.1% acetic acid to promote positive ion formation and were infused directly into the electrospray source (3–4 $\mu\text{L min}^{-1}$). Sample dilutions and spray and instrument parameters were optimized for each sample for maximum spray stability (Kido Soule et al., 2010). Two hundred individual transients were collected and co-added for each sample. In general, the capillary voltage and temperature were 21.0 V and 260°C, respectively. The automatic gain control (AGC) target value was set at 1×10^6 ions for all samples. External mass calibration was conducted weekly with a calibration mix from the manufacturer and the resulting mass accuracy was <2 ppm for $198 < m/z < 2000$. Relative peak height was calculated by normalization to the most abundant ion in the mass spectrum. The average resolving power

was 400,000 at m/z 400 (where resolving power is defined as $m/\Delta m_{50\%}$ where $\Delta m_{50\%}$ is the width at half-height of peak m).

The transients were processed with MATLAB code provided by Southam et al. (2007) and modified as described previously (Kido Soule et al., 2010). Within each sample, only those transients whose total ion current (TIC) was $>20\%$ of the maximal TIC were co-added and then processed with Hanning apodisation and zero-filled once prior to fast Fourier transformation. We retained all m/z values with a signal-to-noise ratio above 5 (as calculated in Southam et al., 2007). All spectra were internally re-calibrated using a short list of m/z values present in all samples, chosen according to criteria previously described (Bhatia et al., 2010). After recalibration, mass accuracy was <1 ppm for our mass range. We removed spectra from consideration if we saw evidence of contamination from the C18 resin (Bhatia et al., 2010). In some spectra, we observed the presence of overlapping features from multiply-charged ions, consistent with published spectra for intact proteins. These features were intermittently present in different samples and replicate filtrates of the same sample. We ascribe these features to whole-cell material that leaked through the combusted Anodisc filters and thus we discarded these spectra as not representative of dissolved organic material. All spectra that were free of contamination and that contained enough m/z values for good calibration (>5 ; Williams and Muddiman, 2007) were retained for further analysis.

The individual sample peak lists were then aligned and combined using MATLAB code provided by Mantini et al. (2007) with an error tolerance of 1 ppm. Elemental formulas were assigned to the aligned peaks (m/z values) using the Compound Identification Algorithm (CIA) (Kujawinski and Behn, 2006; Kujawinski et al., 2009) with the following parameters: (a) formula error was 1 ppm, (b) the relationship error was 20 ppm, and (c) the mass limit above which elemental formulas were assigned by functional group relationships only was 500 Da. For this study, elemental formulas were determined for m/z values below 500 Da with an in-house database of mathematically and chemically legitimate formulae within the 1 ppm error window. These elemental formulas were extended to m/z values above 500 Da through identification of functional group relationships with smaller m/z values. Isotopologs with one or more ^{13}C atoms were annotated and elemental formulas were corrected to reflect ^{13}C content. Elemental ratios and double bond equivalencies (DBE) were calculated as magnitude-averaged values (Sleighter and Hatcher, 2008) for m/z values with assigned elemental formulas. Number-averaged values are normalized to peak diversity and magnitude-averaged values are normalized to both peak diversity and relative peak abundance. Series of ^{13}C -containing isotopologs were calculated using the algorithm described in Weber et al. (2013).

Fragmentation (MS/MS) spectra were generated for selected peaks in the <1.0 - μm samples. Target m/z values were isolated in the ion trap with a 1.0 Da window during direct infusion analysis. Fragmentation occurred in the linear ion trap via collision-induced dissociation (CID) with energies between 16 and 35 (unitless; optimized for each feature), and fragment ions were transferred to the ICR cell for m/z measurement. For all MS/MS

spectra, 100 scans at 100,000 resolving power were co-added and processed as described above for the full spectra. Neutral losses were calculated for each spectrum between each pair of fragments and compared to a list of common neutral losses (Rasche et al., 2011). Fragmentation spectra were also manually compared to entries in MassBank (Horai et al., 2010) and masses of neutral ions and fragments were manually compared to data within METLIN (Tautenhahn et al., 2012). In some cases, initial activation of the precursor ion yielded a secondary ion with twice the original molecular weight, implying that the precursor had been doubly-charged. In these cases, we collected additional fragmentation spectra (MS^3) to examine the structure.

We assessed the possibility that our DOM composition results were biased by material leaching from the 1.0- μm bell filter with a follow-up experiment in January 2013. Freshly collected Vineyard Sound seawater was passed through a 1.0- μm filter that had not been cleaned extensively (as described above), and then filtered again through a 0.2- μm Anodisc. DOM was extracted and compared to DOM from a seawater control that was not passed through the 1.0- μm filter. Overlap between 1.0 μm -filtered and non-filtered seawater samples was $\sim 13\%$, suggesting that the 1.0- μm filter produces significant contamination if not cleaned properly. Approximately 10–20 peaks from the contaminated spectra were observed at moderate abundance in the biological incubations, representing $<1\%$ of the peaks observed in the treatments. The lack of common peaks between this test and our experiment also indicates that the compounds observed in the $<1.0\text{-}\mu\text{m}$ spectra were not associated with a stress response to filtration.

Microbial Parameters

We used flow cytometry and epifluorescence microscopy to quantify the abundances of bacteria and protozoa, respectively. For flow cytometry, paraformaldehyde (0.2% final concentration) was added to 1 mL aliquots and the samples were stored at -80°C until analysis using a Becton-Dickinson FACSCalibur. Autofluorescing cells were quantified against 2.5 μm beads (Molecular Probes). After quantification of autofluorescing cells, SYBR Green I was added to each sample and non-autofluorescing cells were quantified (against 1.0 μm beads—Fluoresbrite plain YG 1.0 μm microspheres). When needed, samples were diluted with ultrapure water prior to analysis. For microscopy, samples (10 mL) were preserved with 1% glutaraldehyde and stored at 4°C for 1–5 days. Cells were then stained with acridine orange and filtered onto 0.2- μm black polycarbonate filters (Hobbie et al., 1977). Protozoa were enumerated by epifluorescence microscopy in at least 75 fields for each filter. The average coefficient of variation for protozoan cell counts was 40%.

Microbial cells were collected at each time point on 0.2 μm Anodisc filters. For each bottle, approximately half the incubation volume ($\sim 1\text{L}$) was filtered at a time and the two resulting filters were used as bottle replicates. All filters were stored at -80°C until DNA extraction. Cells were prepared for digestion through the addition of 500 μL extraction buffer (50 mM Tris-HCl, pH = 8, 40 mM EDTA, 0.75 M sucrose). Lysozyme (0.5 mg) was added and the mixture was incubated at 37°C for 30 min. Proteins were digested with 83 μg proteinase K and 1%

SDS. The mixture was incubated at 65°C for 30 min. DNA was extracted with one volume of phenol and one volume of 25:24:1 phenol: chloroform: isoamyl alcohol. RNA was degraded with RNase cocktail (Ambion) at 37°C for 30 min. DNA was precipitated with 0.1 X volume of 2M LiCl and 2X volume of 100% ethanol. After centrifugation, the DNA pellet was washed twice with cold 70% ethanol and resuspended in 50 μL ultrapure water. DNA concentrations were measured with a Nanodrop spectrophotometer (range: 32–275 $\text{ng } \mu\text{L}^{-1}$, all blanks $<1 \text{ ng } \mu\text{L}^{-1}$). All extracts were stored at -80°C .

The DNA extracts were separated into ^{13}C - and ^{12}C -rich fractions with ultracentrifugation (Longnecker et al., 2009). DNA extracts and TE buffer (10 mM Tris-HCl, pH = 7.5, 1 mM EDTA) were combined to give a total volume of 800 μL and a total DNA content of 1.5 μg . This mixture was then mixed with 4.2 mL of cesium chloride (CsCl) at a density of 1.856 g/mL (refractive index = 1.4143). All tubes were sealed and centrifuged in an ultracentrifuge (Beckman Coulter, Optima L-80 XP) at 200,000 $\times g$ for 65 h at 20°C . After centrifugation, 500- μL aliquots were carefully removed from the top of the tube to the bottom (10 aliquots total) and the refractive index was measured. DNA was then precipitated with polyethylene glycol (30% PEG in 1.6M NaCl) and incubated overnight at 4°C . After centrifugation at 20,000 $\times g$, the DNA pellet was washed three times with cold 70% ethanol, dried, and resuspended in 10 μL of 10 mM Tris. For bacterial rDNA, the quantitative PCR mix consisted of Absolute qPCR mix (ThermoFisherScientific), 200 nM 27F (5'-AGA GTT TGA TCC TGG CTC AG-3') and 200 nM 519R-RT (5'-GWA TTA CCG CGG CKG CTG-3'), ultrapure water and 2 μL of CsCl extract. Amplification proceeded along the following program: hold at 95°C for 15 min; 40 times of hold at 95°C for 15 s, 55°C for 30 s, 72°C for 30 s; hold at 95°C for 15 s; 55°C for 15 s; ramp to 95°C for 30 min; end at 95°C for 15 s. All ultracentrifugation runs contained four sample tubes and two standard tubes. The standards were a 50:50 mixture of ^{12}C -DNA and ^{13}C -DNA extracted from *Halomonas halodurans* grown on uniformly ^{12}C -labeled or ^{13}C -labeled glucose (Barbeau et al., 2001). Based on our previous work with blanks and standard DNA runs (Longnecker et al., 2009), we used a CsCl density of 1.7258 g ml^{-1} as a cut-off between ^{12}C -rich and ^{13}C -rich DNA.

SSU gene copies within CsCl extracts were quantified with quantitative-PCR against a five-point standard curve with *H. halodurans* DNA. For bacterial cells, the DNA extract was amplified with FAM-labeled 27F and 519R primers. The reaction mix was comprised of GoTaq colorless master mix (50% dilution), 200 nM of each primer, bovine serine albumin to increase PCR reaction yield (BSA – 0.25 mg ml^{-1}) and enough ultrapure water to have a total volume of 50 μL per reaction. 16S rDNA PCR amplification used the following program: an initial denaturation (95°C for 5 min) followed by 35 cycles of denaturation (95°C , 30 s), annealing (46°C , 30 s), extension (72°C , 90 s), and a final extension cycle of 72°C for 5 min. All parameters of the 18S reaction mix remained the same except the primers were EukA (5'-AAC CTG GTT GAT CCT GCC AGT-3') and Euk570R (5'-GCT ATT GGA GCT GGA ATT AC-3'). The 18S rRNA gene was amplified according to the program: an initial denaturation (95°C for 2 min) followed by 40 cycles

of denaturation (95°C, 30 s), annealing (50°C, 30 s), extension (72°C, 150 s), and a final extension cycle of 72°C for 7 min. Recoveries of added DNA ranged from 1 to 15%.

The changes in microbial diversity in bulk samples and ultracentrifugation fractions were examined with terminal restriction fragment (TRFs) length polymorphism (TRFLP) analysis of PCR-amplified small subunit ribosomal RNA genes as previously described (Longnecker et al., 2009). Each product was digested with two enzymes, *Hin6I* and *BsuRI* at 37°C for 2 h. After the enzymatic digest, DNA was precipitated from the PCR product mix with 2M LiCl and 100% ethanol. After centrifugation, the pellet was washed twice with cold 70% ethanol, dried and resuspended in HiDi formamide. The lengths of the TRFs were measured with an Applied Biosystems 3730 XL capillary sequencer, relative to a MegaBACE ET900-R size standard. Chromatograms were analyzed with the DAX Data Acquisition and Analysis software and results were exported into MATLAB.

We generated 16S rRNA gene clone libraries for Days 0, 1, 2, and 5 and 18S rRNA gene clone libraries for Days 0, 2, and 5. rRNA genes were cloned using the pCR4-TOPO vector (TOPO-TA, Invitrogen) according to the manufacturer's directions. One 96-well plate of colonies was picked for each gene at each experimental time-point. DNA from the colonies was extracted and sequence data obtained with 27F or EukA. Chimeras were checked with Bellerophon v3. Phylogenetic assignments were conducted with STAP (Wu et al., 2008). Sequences were deposited in GenBank and can be accessed with numbers KC336488-KC337027. Sequence prefixes and corresponding samples are: "Seq7" = Whole Day 0 16S rDNA; "Seq_16" = Whole Day 0 18S rDNA; "p01" = <1.0- μ m Day 1 16S rDNA; "Seq_08" = Whole Day 1 16S rDNA; "p02" = <1.0- μ m Day 2 16S rDNA; "Seq_09" = Whole Day 2 16S rDNA; "Seq13" = Whole Day 2 18S rDNA; "Seq_11" = <1.0- μ m Day 5 16S rDNA; "Seq10" = Whole Day 5 16S rDNA; "Seq_16" = Whole Day 5 18S rDNA.

Statistical Analyses

We considered two data transformations for full spectra and for fragmentation spectra. First, we transformed relative mass spectral peak heights to presence (peak height = 1) or absence (peak height = 0) to assess sample differences based on peak diversity. Second, we considered the original peak heights (no data transformation). For both transformations, a distance matrix was calculated between all the samples using the Bray-Curtis distance measure (MATLAB code by David Jones, personal communication, as part of the Fathom toolbox), and hierarchical cluster analysis was performed using Ward's linkage method.

For all datasets except the fragmentation spectra, non-metric multidimensional scaling (NMS) analyses were conducted with the statistics toolbox in MATLAB. We chose two dimensions based on Monte Carlo analysis. The proportion of variation represented by each axis was assessed with a Mantel test that calculates the coefficient of determination (r^2) between distances in the ordination space and in the original space. One-way analysis of similarity (ANOSIM) was used to assess if groups

visualized by NMS were statistically significant. MATLAB code for ANOSIM was also from the Fathom toolbox. The Bray-Curtis distance matrix calculated for the NMS was used for ANOSIM, and the distances were converted to ranked distances prior to ANOSIM calculations. The significance of each group was tested by 1000 randomizations of the dataset, and p -values were calculated to determine the probability of no difference between groups.

For the full mass spectra, we identified specific m/z values characteristic of the observed cluster groupings with Indicator Species Analysis (ISA). The separation of samples into ISA groups and the curation of indicator m/z values was conducted according to previously described criteria (Kujawinski et al., 2009). Our samples were separated into two groups: Group 1 = whole water incubations; Group 2 = <1.0- μ m incubations. ISA combines the relative abundance and relative frequency of a peak within a pre-defined group of samples to assign an indicator value (IV) to each peak (McCune and Grace, 2002). A perfect IV (equal to 100) of a particular group would constitute an m/z value that was present exclusively in the samples comprising that group (McCune and Grace, 2002), however an IV threshold of 50 was used to assign groups (Kujawinski et al., 2009). Statistical significance of IVs is calculated by comparison with Monte-Carlo simulations of randomized data ($p < 0.05$).

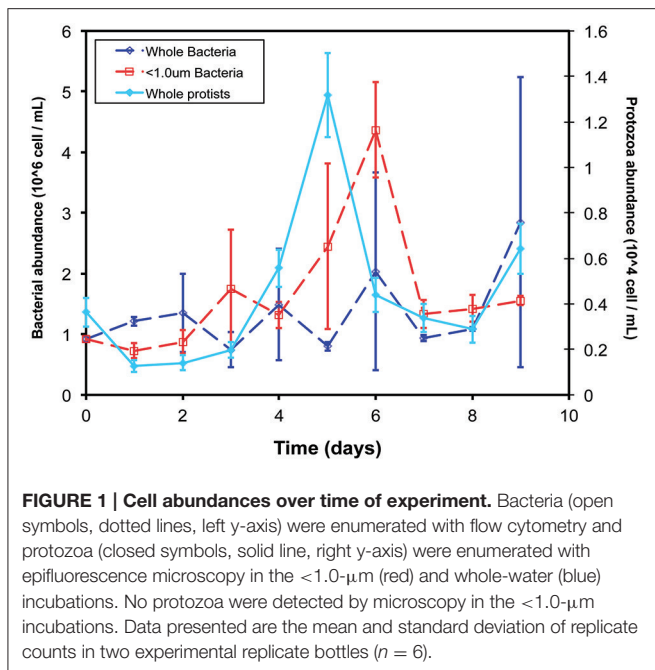
RESULTS

General Overview

Bacterial abundance increased in the <1.0- μ m incubations after the addition of isotopically-labeled glucose but remained constant in the whole-water incubations (Figure 1). In the whole-water treatments, we quantified protozoa and auto-fluorescing cells. The number of auto-fluorescent (phytoplankton) cells was negligible at all time points. In these treatments, protozoa peaked in abundance on day 5, and were never detected microscopically in the <1.0- μ m incubations (Figure 1).

Stable Isotope Incorporation

We assessed the degree of stable isotope incorporation in both the DOM and microbial analyses. In the DNA measurements, isotopic incorporation was sufficiently large to allow separation of isotopically-labeled DNA from bulk DNA by ultracentrifugation (see below). In contrast, little incorporation was observed in the DOM fraction. Using algorithms from Weber et al. (2013), we identified series of peaks containing more than one ^{13}C atom only in the <1.0- μ m spectra (Table S1). No such series were found in the whole water incubations. According to Weber et al. (2013), the longer series could indicate increased ^{13}C incorporation. However, this conclusion must be confirmed by elemental formula calculations. Using the formula from Koch et al. (2007), the carbon number predicted from the relative intensities of these peaks was approximately the same as that predicted from the exact mass of the primary ion. Thus, no enhanced incorporation could be assumed and we must conclude that the increased series lengths are due instead to the large intensities of the parent ions. Indeed, the ions annotated as the start of the longer series are among the most abundant ions in

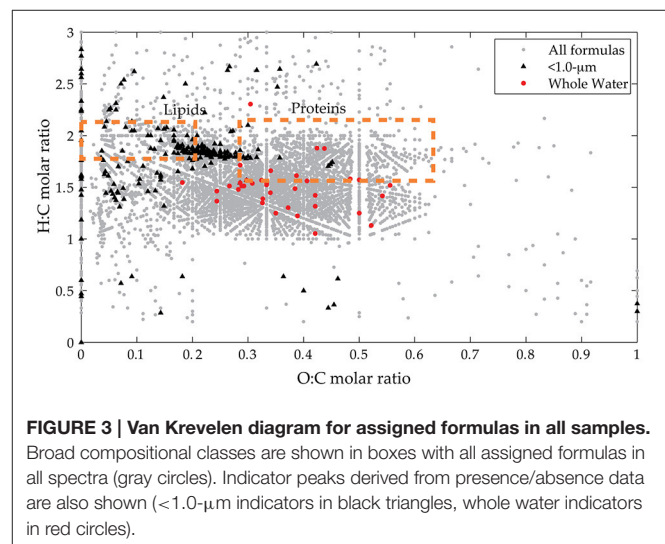
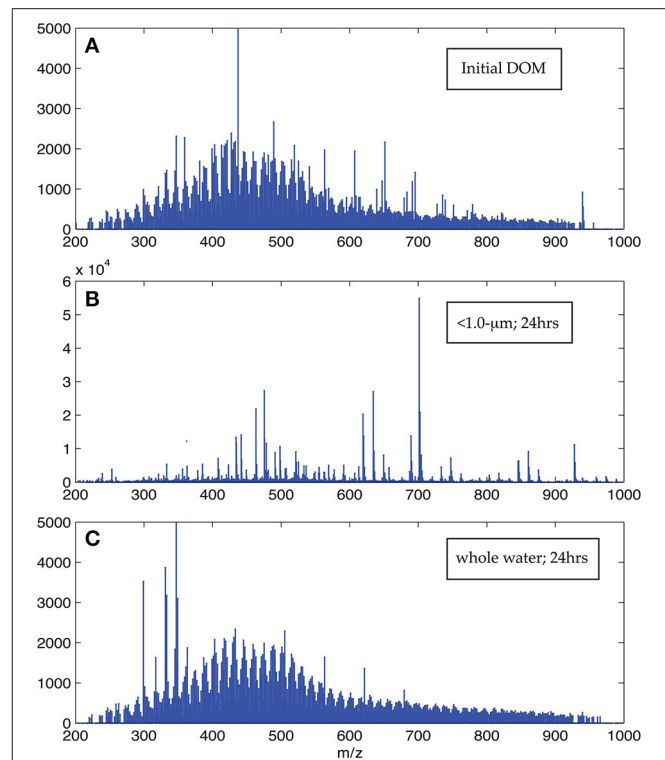


the <1.0- μm spectra. We conclude that isotopic incorporation of ^{13}C from glucose could not be clearly discerned in the DOM in this experiment, and further discussion focuses on glucose as a carbon source, rather than on ^{13}C as a tag for recent biological synthesis.

DOM Composition

The visual difference between ultrahigh resolution mass spectra from the <1.0- μm and the whole water incubations is striking (Figure 2). The <1.0- μm spectra are not contaminated with bleed from the filter, based on blank tests conducted after this experiment. Thus, we conclude that the unique peaks in these spectra are due to biological activity within this treatment. In contrast, the mass spectra from the initial seawater and the whole water incubations are consistent with previous spectra of coastal DOM (Sleighter and Hatcher, 2008), both in terms of formula composition and magnitude-averaged bulk parameters (Table 1). Elemental formulas were assigned to the majority of peaks in all spectra (range: 79–99%; Table 2). Formulas with CHO were the most numerous formula class in all DOM samples but minor contributions from heteroatoms such as N and S were also observed (Tables 1, 2). The high-abundance peaks in the <1.0- μm spectra have a unique composition relative to the initial DOM and occur throughout the spectrum (Figure 3). These peaks shift the bulk parameters toward higher contributions of N and S and lower aromaticities as quantified by DBE values (Table 1).

Cluster analysis (Figure 4A) and NMS (Figure 4B) of the full-scan MS data confirm the visual difference between whole water and <1.0- μm incubations. The primary separation in both statistical analyses is size fractionation, presumably due to removal of larger organisms by the 1.0- μm filter. The DOM from whole water incubations occurs in a tight group with the



initial coastal DOM in both the cluster analysis and the NMS ordination, reflecting minor variability in peak diversity among these samples. The DOM samples from <1.0- μm treatments are more variable between biological replicates and exhibit greater distances in the dendrogram (Figure 4A) and more scatter in

TABLE 1 | Elemental ratios for all samples, calculated as magnitude-averaged values (Sleighter and Hatcher, 2008) for m/z values with assigned elemental formulas.

Incubation	Day	H:C _w	O:C _w	N:C _w	S:C _w	DBE _w
Initial	0	1.45	0.33	0.035	0.0007	8.1
Whole water	1	1.47, 1.42	0.34, 0.33	0.045, 0.022	0.0008, 0.0004	8.2, 8.7
	2	1.46	0.33	0.032	0.0005	8.3
	5	1.42	0.35	0.028	0.0002	8.7
	9	1.42	0.30	0.034	0.0008	8.0
<1.0- μm	1	1.45, 1.40	0.20, 0.25	0.13, 0.084	0.022, 0.019	5.7, 6.7
	2	1.47	0.18	0.14	0.029	5.6
	5	1.41, 1.39	0.25, 0.23	0.090, 0.10	0.014, 0.016	6.9, 6.7
	9	1.43	0.26	0.089	0.014	6.8

Values from experimental replicate spectra are shown as two values within the same time point. Initial values are consistent with previous determinations in coastal seawater (Sleighter and Hatcher, 2008).

TABLE 2 | Formula classes for each mass spectrum.

Incubation	Day	# peaks	Overlap	# formulas	CHO	CHON	CHOS	CHONS	Other
NUMBER-AVERAGED									
Initial	0	2813	—	2759 (98%)	83.6	8.4	0.8	0.5	6.2
Whole water	1A	2787	2202 (79%)	2719 (98%)	81.1	8.6	0.2	1.0	8.4
	1B	2916	2252 (77%)	2884 (99%)	82.7	7.9	0.2	0.5	8.4
	2	2537	2120 (84%)	2496 (98%)	84.4	7.3	0.1	0.8	7.2
	5	2145	1801 (84%)	2131 (99%)	83.2	6.2	0.0	0.0	10.4
	9	2771	2157 (78%)	2689 (97%)	83.5	7.8	1.2	0.5	6.7
<1.0- μm	1A	2289	1077 (47%)	1883 (82%)	55.3	29.7	1.3	5.3	5.9
	1B	2792	1868 (67%)	2526 (90%)	72.4	15.0	0.8	3.2	7.2
	2	2567	834 (32%)	2038 (79%)	44.5	36.5	1.8	7.0	7.3
	5A	2653	1823 (69%)	2419 (91%)	73.5	15.4	1.3	2.5	6.0
	5B	3101	1868 (60%)	2731 (88%)	69.9	17.4	0.8	2.8	7.6
	9	2931	1855 (63%)	2670 (91%)	70.5	17.5	0.5	2.8	7.4
MAGNITUDE-AVERAGED									
Initial	0				87.6	5.7	0.4	0.2	4.3
Whole water	1A				84.0	7.0	0.1	0.6	5.9
	1B				89.2	3.9	0.1	0.2	5.2
	2				88.5	5.2	0.1	0.4	4.5
	5				86.7	4.0	0.0	0.0	7.2
	9				85.7	4.1	0.6	0.3	6.1
<1.0- μm	1A				24.4	44.5	1.1	8.0	3.4
	1B				50.9	25.4	0.8	5.0	3.9
	2				15.0	49.1	1.2	10.7	4.0
	5A				53.5	24.6	0.9	5.1	3.6
	5B				45.1	27.3	0.3	4.8	5.6
	9				51.4	26.7	0.3	5.1	3.7

The overlap column contains the number of peaks in that spectrum that were present in the initial seawater spectrum (% provided based on peak number in preceding column). Number- and magnitude-averaged values determined by equations from Sleighter and Hatcher (2008). Replicate samples are denoted by A or B.

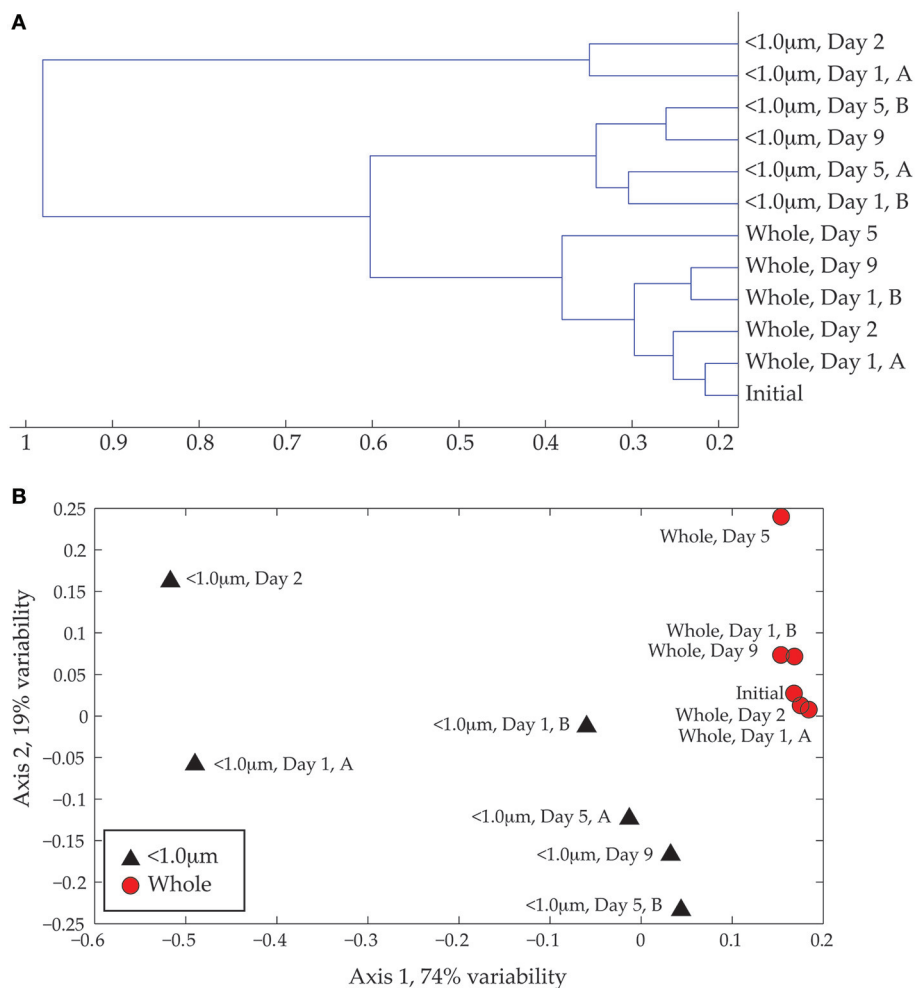


FIGURE 4 | (A) Cluster analysis of ESI FT-ICR positive-ion mode mass spectra. Similarities among spectra were assessed using the Bray-Curtis distance matrix calculated with presence/absence data. **(B)** Non-metric multidimensional scaling (NMS) ordination of same data. The $<1.0\text{-}\mu\text{m}$ and the whole water data are shown with black triangles and red circles, respectively. The degree of variability represented by each axis was calculated using a Mantel test (see text) and is shown in the axis label. The stress for this ordination is 0.029 and the r^2 is 0.94.

the NMS ordination (**Figure 4B**). The separation between the whole-water and $<1.0\text{-}\mu\text{m}$ incubations is statistically significant (ANOSIM: $R = 0.5926$, $p = 0.001$). There does not appear to be a significant impact of incubation time on DOM composition, although we may not have sufficient data to fully constrain this effect.

The indicator MS peaks for the two pre-assigned groups (whole water and $<1.0\text{-}\mu\text{m}$) have distinct compositional signatures (**Figure 3**; Table S1). The whole water indicators occur in the region characteristic of marine refractory DOM (e.g., Sleighter and Hatcher, 2008; Kujawinski et al., 2009) that contains aromatic or alicyclic oxidized moieties. This material is considered to be the product of extensive reworking and humification reactions (Hertkorn et al., 2006) and thus is unlikely to represent recently-synthesized biomass. We hypothesize that these indicator values represent refractory DOM molecules whose ionization is suppressed in the $<1.0\text{-}\mu\text{m}$ samples. In contrast, the bacterial indicators have high H:C and

low-to-moderate O:C ratios, similar to the lipid-like and protein-like regions of the van Krevelen diagram. In addition, they have elevated N and S content and appear to be more aliphatic with lower DBE values. We hypothesize that the $<1.0\text{-}\mu\text{m}$ indicators represent compounds produced by bacterial metabolism, even though they are not isotopically-enriched.

The ultrahigh mass resolution of the FT-ICR MS used here allowed us to resolve individual molecules produced in the $<1.0\text{-}\mu\text{m}$ treatments and to probe their structural composition with MS/MS. This ability is unusual in DOM compositional studies because, in most cases, >10 peaks share a nominal mass and they cannot be adequately separated for MS/MS fragmentation. However, the $<1.0\text{-}\mu\text{m}$ indicator molecules often dominated their nominal mass windows and sufficiently high abundances of an individual feature could be isolated within the ion-trap for fragmentation. Twenty-two indicator m/z values were selected based on relative abundance in all $<1.0\text{-}\mu\text{m}$ samples (Table S1). None of the fragmentation spectra yielded matches within

associated with neutral losses (Figure S3). The largest group of common spectra exhibited high numbers of N-containing neutral losses, including the putative peptide moieties (Figure 5 and Figure S3). Since the precursor molecules do not match any peptides in METLIN, it is unlikely that these molecules are peptides themselves but they may have peptide side chains or other peptidic functional groups. Another group of spectra exhibited high numbers of O-containing neutral losses (Figures S1, S3). These functionalities are common in biomolecules and thus do not provide sufficient information to propose compound structure or biological function. Future annotation or identification of these molecules may be possible as mass spectral databases of microbial metabolites are further populated.

Microbial Diversity

The primary treatment in this experiment was the removal of organisms $>1.0\ \mu\text{m}$ in diameter, i.e., eukaryotic phytoplankton, protozoan grazers, and particle-associated bacteria. We examined microbial diversity microscopically and using TRFLP and clone libraries. Microscopic investigations showed a minimal contribution of auto-fluorescing cells to the whole water incubations while protozoan abundances increased. Thus, we attribute the bulk of our biological and chemical signals to protozoan grazing activity.

We observed similar results between the TRFLP data generated by the two enzymes (*Hin6I* and *BsuRI*) and, for brevity, we present only the data from the *Hin6I* enzyme cleavage. NMS ordination of this data shows that the bacterial diversity in the $<1.0\text{-}\mu\text{m}$ and the whole-water incubations is distinct in the bulk DNA extracts (Figure 6; ANOSIM: $R = 0.6366$, $p = 0.001$). The clone library data suggests that this difference is due to the prevalence of Bacteroidetes and γ -proteobacteria in the $<1.0\text{-}\mu\text{m}$ treatments relative to α -proteobacteria in the whole water incubations (Table S2 and Figure 7). Rarefaction analysis of our clone library data suggests that we did not fully capture the diversity of bacteria in our incubations.

The TRFLP data from the CsCl fractions confirmed the large influence of $>1.0\text{-}\mu\text{m}$ organisms on bacterial diversity (Figure 8A; ANOSIM: $R = 0.3592$, $p = 0.001$). We also examined the diversity in ^{13}C -rich fractions (i.e., “metabolically active”) relative to ^{13}C -poor fractions (i.e., “metabolically inactive”) to assess the impact of added substrate on bacterial diversity in both treatments. The active and inactive TRFs separate along the second axis (Figure 8B; ANOSIM: $R = 0.1894$, $p = 0.001$). The distinction is statistically significant even though the variability explained along the second axis is lower (12% on Axis 2 vs. 70% on Axis 1) and the ANOSIM results are less definitive. It should be noted that the separation is driven primarily by data from the early time points and comparatively fewer TRFs were found in the “metabolically active” region on Day 9. This is likely due to increasing remineralization of the added glucose to carbon dioxide and overall decrease in isotopic content in the incubations. Samples to confirm this hypothesis were lost during analysis.

No cells larger than $1.0\text{-}\mu\text{m}$ were detected by microscopy in the $<1.0\text{-}\mu\text{m}$ incubations; therefore, we restricted the following 18S rDNA diversity analyses to the whole water incubations. The

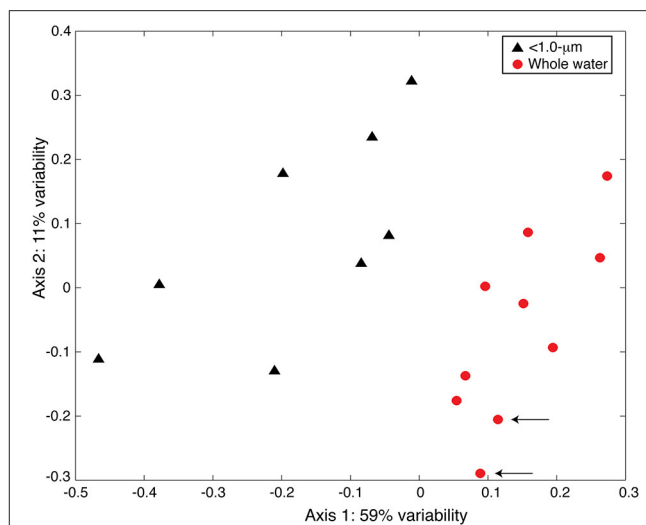
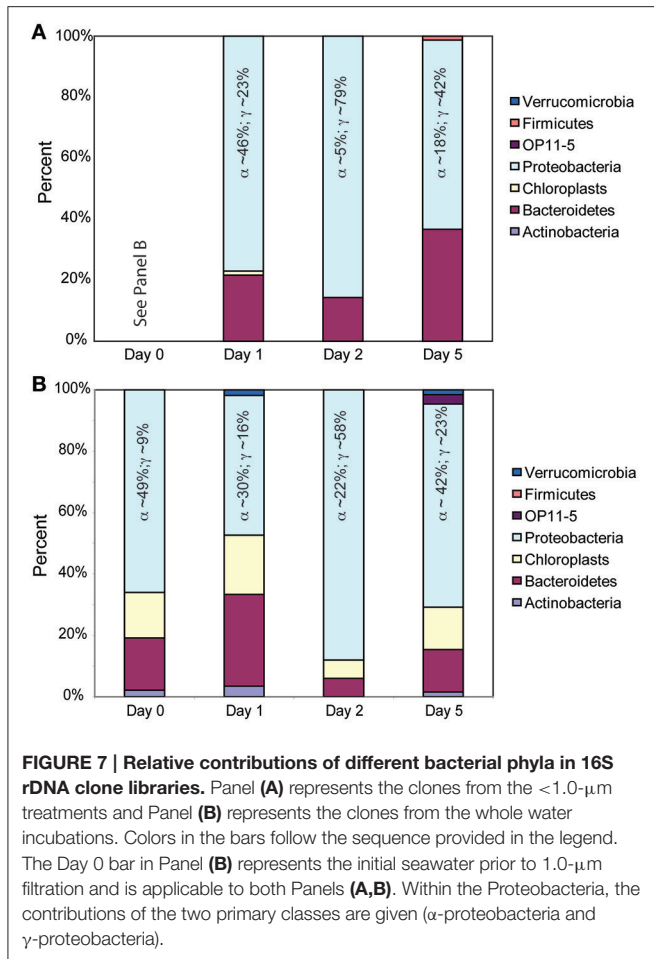


FIGURE 6 | NMS ordination of 16S rDNA TRFLP samples (*Hin6I*). The $<1.0\text{-}\mu\text{m}$ (black triangles) and the whole water (red circles) incubations are presented. The stress for this ordination is 0.124 and the r^2 between the original distance matrix and this NMS ordination is 0.90. The degree of variability represented by each axis was calculated using a Mantel test (see text) and is shown in the axis label. Arrows indicate samples from the original seawater.

NMS ordination of 18S rDNA from the CsCl fractions shows no statistically significant difference between “metabolically active” and “metabolically inactive” TRFLP samples (Figure 9; ANOSIM: $R = 0.0589$, $p = 0.1060$). However, there are “metabolically active” TRFs in the NMS ordination that may reflect grazing of labeled bacteria, or the uptake of isotopically-labeled DOM (outside our analytical window). Although we did not determine the identity of these TRFs, the presence of “metabolically active” TRFs and our microscopy results, which show an increase in nanoflagellate abundance over the time course of our experiment, support the notion that grazing of prey occurred in our experiments. The sequences collected in our bulk 18S rDNA clone libraries (Table S3) confirm the presence of common protozoan bacterivores (ciliates, dinoflagellates, and stramenopiles; Jürgens and Massana, 2008).

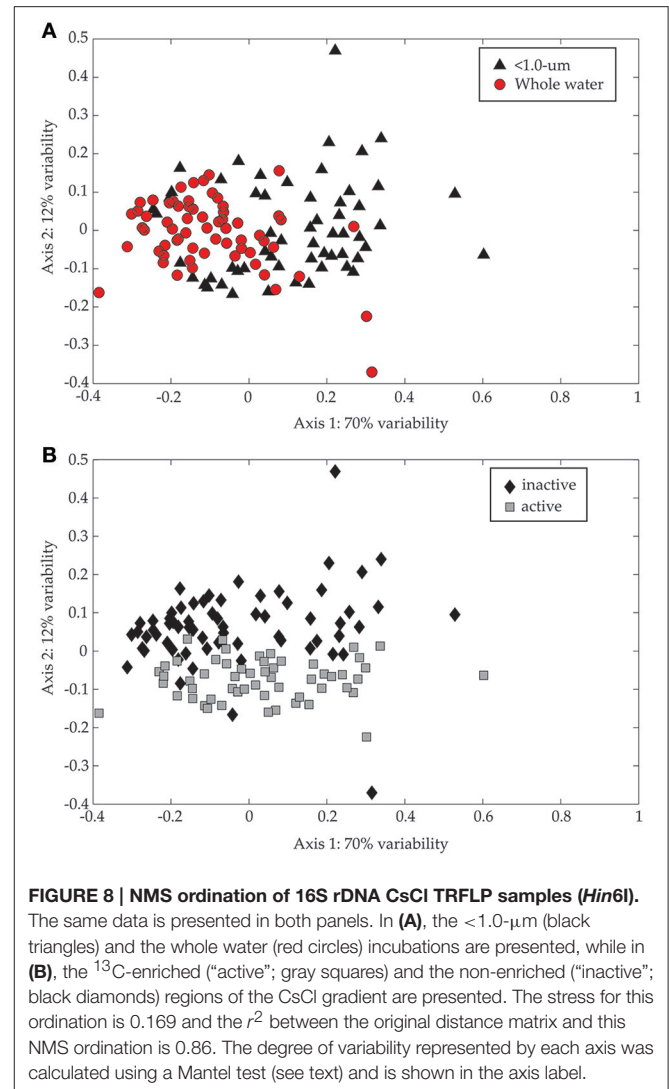
DISCUSSION

This study provides an opportunity to simultaneously evaluate bacterial diversity and DOM composition as a function of the presence or absence of larger organisms, including protozoan grazers. Although the role of bacterial diversity in DOM composition has been investigated in numerous studies (reviewed in Kujawinski, 2011), experiments have only recently been able to include molecular-level details on DOM composition using ultrahigh resolution mass spectrometry (e.g., Arrieta et al., 2015; Lechtenfeld et al., 2015; Pedler Sherwood et al., 2015). In addition, these investigations commonly exclude large phytoplankton and protozoan grazers by dilution or filtration. The purpose of our study was to combine assessments of biological and chemical



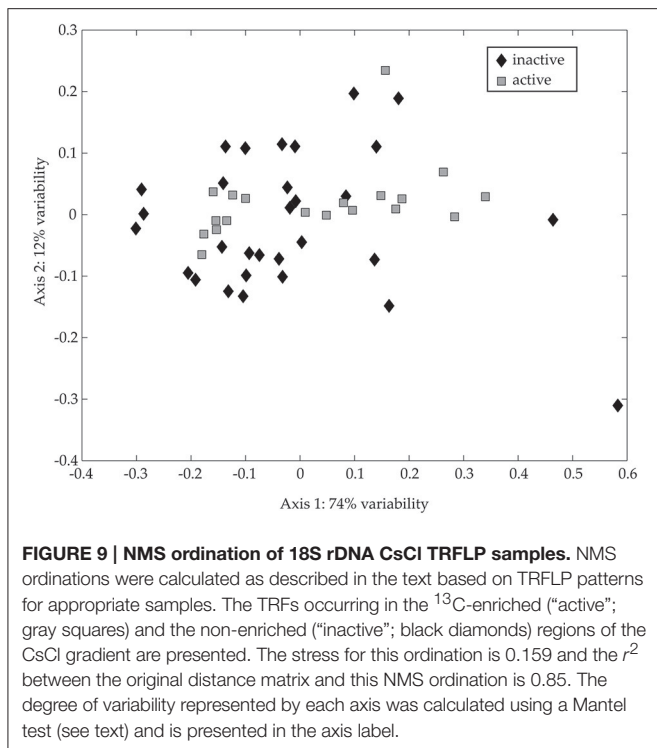
diversity to understand the relative impacts of multiple trophic levels on both bacterial community structure and DOM composition.

In the initial seawater, the bacterial community is consistent with prior assessments of coastal bacterial diversity (Mou et al., 2008) and the relative contributions of Bacteroidetes, α -proteobacteria, and γ -proteobacteria clones increase after glucose addition (Figure 7). This shift in diversity is consistent with previous reports of glucose utilization among coastal bacteria (Allers et al., 2007; Alonso-Sáez et al., 2009), bacterial response to organic matter pulses from phytoplankton blooms (Eiler and Bertilsson, 2007) and enclosure experiments with elevated nutrients (Fouilland et al., 2014; Baltar et al., 2016). The γ -proteobacteria, in particular, grow rapidly when glucose is added and are highly susceptible to grazing by heterotrophic nanoflagellates (Alonso-Sáez et al., 2009). The enhanced presence of Bacteroidetes clones in the <1.0- μm incubations may be due to this clade's ability to degrade complex organic matter (Cottrell and Kirchman, 2000) and/or to predate on other bacteria (Banning et al., 2010). Nevertheless, bacterial diversity and DOM composition were not correlated (Mantel test, $p > 0.05$). Thus, we cannot assign specific DOM exudates to bacterial groups identified in the clone libraries, possibly reflecting the "generalist"



behavior of coastal bacteria to pulse nutrient additions (Mou et al., 2008). Instead, the presence of larger organisms, including protozoa, appears to overwhelm the impacts of substrate addition on community diversity.

DOM composition in the two treatments was visually and statistically distinct. The <1.0- μm incubations had DOM with a unique composition from the unfiltered, whole water, incubations, and we posit that these differences are due to increased bacterial abundance and altered bacterial physiology in the absence of grazing. Together these differences might correspond to shifts in the composition of bacterial-derived DOM or exudates. Although the composition of bacterial-derived DOM is not well-constrained across different bacterial clades (Carlson, 2002), it has been shown to contain membrane and cell wall components, including peptidoglycan (Stodereger and Herndl, 1998), and it may be refractory on short- to medium-time scales (days to months; Ogawa et al., 2001; Kawasaki and Benner, 2006). The elemental composition of material in our incubations is consistent with lipid-like and



protein-like compounds and fragmentation spectra indicate the presence of numerous peptide moieties. Thus, the overall characteristics of the features in our <1.0- μ m dataset are consistent with those assumed for bacterial-derived DOM. To test the hypothesis that the compounds observed in the <1.0- μ m incubations were derived from bacterial cell walls, we compared our data to published peptidoglycan structures (Schleifer and Kandler, 1972). Although we found no matches between our data and published structures, the structure of the peptide bridge in peptidoglycan is quite variable (Schleifer and Kandler, 1972) and amino acids are present in a variety of other bacterial exudate molecules (Kaiser and Benner, 2008). Nevertheless, the fact that these molecules were not detected in the whole water incubations suggests that they are produced as a response to high bacterial densities or to a release from grazing pressure. The MS/MS spectra, together with the exact masses, provide the basis for future development of quantitative MS methods that could probe the roles and dynamics of these compounds within bacteria-rich microenvironments such as biofilms.

This lipid-/peptide-like material may have been produced solely by a subset of bacteria in the <1.0- μ m incubations. This could include opportunistic γ -proteobacteria dominant in the early time points. It is also possible that bacteria in the <1.0- μ m incubations were limited by nutrients (e.g., phosphorus) and increased or altered their exudate compositions. However, these hypotheses are unlikely to be correct because the lipid-/peptide-like material was never observed in the whole water DOM and γ -proteobacteria clones were prevalent in the early time-points of both incubations. Furthermore, this material was present

uniformly across all time points in the <1.0- μ m incubation, rather than as a result of increasing nutrient limitation. An alternative explanation is that the organisms in the whole water incubations (larger than 1.0- μ m) consumed the lipid-/peptide-like material directly. This hypothesis is not realistic because the protozoa or phytoplankton would have had to consume this material entirely without leaving any trace for ionization. This seems unlikely given the amount of material evident in the <1.0- μ m incubations and its apparently high ionization efficiency. This hypothesis is also inconsistent with previous findings (Gruber et al., 2006) where protozoa did not consume the DOM produced by bacteria. For all of these hypotheses, the lack of this material in the first time point (24 h) of the whole water incubations suggests that it was simply not produced in this incubation. The most likely explanation is that the physiology of bacteria was altered in the <1.0- μ m incubations, relative to the whole water incubations, enhancing the production of distinct DOM molecules. Bacteria are known to produce extracellular material that can be surface-associated (Stoderegger and Herndl, 1998) and/or enriched in carbohydrate moieties (extracellular polysaccharides; Passow, 2002). Further, surface properties of bacteria can change as a function of grazing pressure (Matz and Jürgens, 2003), which could lead to compositional or dynamic shifts in released DOM.

In the whole water incubations, we looked for signatures of molecules that could be assigned to the organisms removed by the 1.0- μ m filter, such as large phytoplankton and nanoflagellate protozoan grazers. Phytoplankton exudates are not well constrained, although they have been shown to contain numerous compounds, including amino acids and polysaccharides, none of which were observed in our spectra. However, as noted above, we observed few auto-fluorescent cells on our microscopy filters and the 18S rDNA clone libraries contain representatives of common protozoan grazing clades observed in coastal seawater. Thus, we infer that the primary active organisms in this size class were protozoa, grazing on bacterial prey. Previous work suggests that protozoa can have a large, indirect, impact on bulk DOM concentrations (Nagata and Kirchman, 1992; Strom et al., 1997). Some authors have proposed that protozoan grazing may be the primary source of DOM in oligotrophic regions (Jumars et al., 1989; Nagata, 2000). Past studies of protozoan egesta have observed small molecules such as amino acids or urea (Andersson et al., 1985; Nagata and Kirchman, 1991) or colloidal material (Taylor et al., 1985; Nagata, 2000). Both of these compound classes fall outside our analytical window ($200 < m/z < 1000$); individual amino acids (and urea) are too small and colloidal materials (1–10 kDa) are too large. Therefore, we cannot clearly distinguish these putative grazing products in the whole-water DOM, consistent with the other two mass spectrometry-based investigations of protozoan-derived DOM (Kujawinski et al., 2004; Gruber et al., 2006) and past observations by Taylor et al. (1985) of limited impact of grazing on the 500–1000 Da size fraction. Recent experiments observed production of labile (Fouilland et al., 2014) or humic-/ protein-like material (Baña et al., 2014) during protozoan grazing. Our results would be consistent with these previous studies if the material produced is colloidal and contains protein-like moieties.

However, the nature of this material could be very different structurally and further experiments are needed to constrain the size and molecular composition of colloidal protozoan egesta.

We also compared the *m/z* features in the whole water incubations to the compound data in KEGG in order to test whether cellular components were present in these incubations. We found no significant overlap, suggesting the lack of common cytoplasm components in this DOM, or the rapid consumption of these molecules leading to exceedingly low concentrations. These data do not definitively prove that no cellular DOM was present, but instead suggest that these components are difficult to discern against the background DOM. Emerging tools in metabolomics that separate individual molecules or classes from background DOM hold great potential for isolating new proxies of phytoplankton exudates and grazing in complex mixtures (Kido Soule et al., 2015; Longnecker et al., 2015a). Application of these tools to the questions posed here will be an important step forward in identifying compounds that could serve as markers in the field for trophic interactions.

The striking difference between DOM composition in our two treatments highlights the potential artifacts that can arise when a microbial community is modified for detailed experimentation. The bottle incubations in this study altered the microbial communities relative to the initial seawater but the DOM composition data suggests that the presence of organisms >1.0- μm mitigated this impact. We posit that the refractory DOM produced in past studies could reflect the absence of some community members, such as grazers, rather than a ubiquitous capability of heterotrophic bacterial metabolism. Indeed the difference in DOM composition between the two treatments suggests that the net metabolism of a community differs fundamentally from the metabolism of individual fractions. Thus, incomplete, or possibly inaccurate, assessments of organism traits and metabolic capabilities could develop when studies exclude common co-occurring microbes, such as protozoan predators. Similar concerns arise in incubations that exclude slow-growing archaea (Santoro and Casciotti, 2011) or low-abundance zooplankton such as copepods (Steinberg et al., 2004). The impacts of many of these organisms on the marine carbon cycle may be underappreciated due to their incompatibility with standard, tractable,

laboratory, and field experiments. Using tools such as those described here would enable the identification of a chemical footprint of these organisms and subsequent assessment of their quantitative contribution to marine DOM. In general, additional work is needed to fully characterize the material produced in marine ecosystems, with a focus on labile molecules that fuel carbon turnover. The sensitivities of microbial consortia to anticipated climate changes are poorly constrained and thus remain an open question for biogeochemical modeling efforts for future ocean scenarios. In particular, identification and quantification of proxies for grazing and other mortality processes, as well as estimates of their remineralization rates, could prove important to disentangling the relative impact of carbon release from organisms in larger size classes and/or higher trophic levels.

AUTHOR CONTRIBUTIONS

EK designed the study, analyzed the data, and wrote the paper; KL, RW, and MK contributed new analytical tools; KL and KB completed the lab work; all authors edited the paper.

ACKNOWLEDGMENTS

Funding for the work was provided by the National Science Foundation (CAREER-OCE-0529101 and OCE-0928424 to EK). The mass spectral data was collected at the WHOI FT-MS Facility which was funded by the National Science Foundation (OCE-0619608) and the Gordon and Betty Moore Foundation. The authors are grateful to Louisa Morrison for early technical assistance, to Benjamin Van Mooy for the use of the DAX software, to Rebecca Gast and Mark Dennett for assistance with the flow cytometer, to Gretchen Swarr for assistance in the lab, and to past and present members of the Kujawinski group for critical comments on the manuscript.

SUPPLEMENTARY MATERIAL

The Supplementary Material for this article can be found online at: <http://journal.frontiersin.org/article/10.3389/fmars.2016.00045>

REFERENCES

- Allers, E., Gómez-Consarnau, L., Pinhassi, J., Gasol, J. M., Šimek, K., and Pernthaler, J. (2007). Response of Alteromonadaceae and Rhodobacteriaceae to glucose and phosphorus manipulation in marine mesocosms. *Environ. Microbiol.* 9, 2417–2429. doi: 10.1111/j.1462-2920.2007.01360.x
- Alonso-Sáez, L., Sánchez, O., and Gasol, J. M. (2012). Bacterial uptake of low molecular weight organics in the subtropical Atlantic: are major phylogenetic groups functionally different? *Limnol. Oceanogr.* 57, 798–808. doi: 10.4319/lo.2012.57.3.0798
- Alonso-Sáez, L., Unanue, M. A., Latatu, A., Azua, I., Ayo, B., Artolozaga, I., et al. (2009). Changes in marine prokaryotic community induced by varying types of dissolved organic matter and subsequent grazing pressure. *J. Plankton Res.* 31, 1373–1383. doi: 10.1093/plankt/fbp081
- Amin, S. A., Parker, M. S., and Armbrust, E. V. (2012). Interactions between diatoms and bacteria. *Microbiol. Mol. Biol. Rev.* 76, 667–684. doi: 10.1128/MMBR.00007-12
- Andersson, A., Lee, C., Azam, F., and Hagstrom, A. (1985). Release of amino acids and inorganic nutrients by heterotrophic marine microflagellates. *Mar. Ecol. Prog. Ser.* 23, 99–106. doi: 10.3354/meps023099
- Arrieta, J. M., Mayol, E., Hansman, R. L., Herndl, G. J., Dittmar, T., and Duarte, C. M. (2015). Dilution limits dissolved organic carbon utilization in the deep ocean. *Science* 348, 331–333. doi: 10.1126/science.1258955
- Azam, F., Fenchel, T., Field, J. G., Gray, J. S., Meyer-Reil, L. A., and Thingstad, F. (1983). The ecological role of water-column microbes in the sea. *Mar. Ecol. Prog. Ser.* 10, 257–263. doi: 10.3354/meps010257
- Baltar, F., Palovaara, J., Unrein, F., Catala, P., Horňák, K., Šimek, K., et al. (2016). Marine bacterial community structure resilience to changes in protist

- predation under phytoplankton bloom conditions. *ISME J.* 10, 568–581. doi: 10.1038/ismej.2015.135
- Baña, Z., Ayo, B., Marrasé, C., Gasol, J. M., and Iriberrí, J. (2014). Changes in bacterial metabolism as a response to dissolved organic matter modification during protozoan grazing in coastal Canabrian and Mediterranean waters. *Environ. Microbiol.* 16, 498–511. doi: 10.1111/1462-2920.12274
- Banning, E. C., Casciotti, K. L., and Kujawinski, E. B. (2010). Novel strains isolated from a coastal aquifer suggest a predatory role for *Flavobacteria*. *FEMS Microbiol. Ecol.* 73, 254–270. doi: 10.1111/j.1574-6941.2010.00897.x
- Barbeau, K. A., Kujawinski, E. B., and Moffett, J. W. (2001). Remineralization and recycling of iron, thorium and organic carbon by heterotrophic marine protists in culture. *Aquat. Microb. Ecol.* 24, 69–81. doi: 10.3354/ame024069
- Becker, J. W., Berube, P. M., Follett, C. L., Waterbury, J. B., Chisholm, S. W., DeLong, E. F., et al. (2014). Closely related phytoplankton species produce similar suites of dissolved organic matter. *Front. Microbiol.* 5:111. doi: 10.3389/fmicb.2014.00111
- Bhatia, M. P., Das, S. B., Charette, M. A., Longnecker, K., and Kujawinski, E. B. (2010). Molecular characterization of dissolved organic matter associated with the Greenland ice sheet. *Geochim. Cosmochim. Acta* 74, 3768–3784. doi: 10.1016/j.gca.2010.03.035
- Carlson, C. A. (2002). “Production and removal processes,” in *Biogeochemistry of Marine Dissolved Organic Matter*, eds D. A. Hansell and C. A. Carlson (San Diego, CA: Elsevier Science), 91–152.
- Corno, G., and Jürgens, K. (2008). Structural and functional patterns of bacterial communities in response to protist predation along an experimental productivity gradient. *Environ. Microbiol.* 10, 2857–2871. doi: 10.1111/j.1462-2920.2008.01713.x
- Cottrell, M. T., and Kirchman, D. L. (2000). Natural assemblages of marine proteobacteria and members of the Cytophaga-Flavobacter cluster consuming low- and high-molecular-weight dissolved organic matter. *Appl. Environ. Microbiol.* 66, 1692–1697. doi: 10.1128/AEM.66.4.1692-1697.2000
- Durham, B. P., Sharma, S., Luo, H., Smith, C. B., Amin, S. A., Bender, S. J., et al. (2015). Cryptic carbon and sulfur cycling between surface ocean plankton. *Proc. Natl. Acad. Sci. U.S.A.* 112, 453–457. doi: 10.1073/pnas.1413137112
- Eiler, A., and Bertilsson, S. (2007). *Flavobacteria* blooms in four eutrophic lakes: Linking population dynamics of freshwater bacterioplankton to resource availability. *Appl. Environ. Microbiol.* 73, 3511–3518. doi: 10.1128/AEM.02534-06
- Fouilland, E., Tolosa, I., Bonnet, D., Bouvier, C., Bouvier, T., Bouvy, M., et al. (2014). Bacterial carbon dependence on freshly produced phytoplankton exudates under different nutrient availability and grazing pressure conditions in coastal marine waters. *FEMS Microbiol. Ecol.* 87, 757–769. doi: 10.1111/1574-6941.12262
- Gruber, D. F., Simjouw, J.-P., Seitzinger, S. P., and Taghon, G. L. (2006). Dynamics and characterization of refractory dissolved organic matter produced by a pure bacterial culture in an experimental predator-prey system. *Appl. Environ. Microbiol.* 72, 4184–4191. doi: 10.1128/AEM.02882-05
- Hedges, J. I. (2002). “Why dissolved organics matter,” in *Biogeochemistry of Marine Dissolved Organic Matter*, eds D. A. Hansell and C. A. Carlson (San Diego, CA: Elsevier Science), 1–34.
- Hertkorn, N., Benner, R., Frommberger, M., Schmitt-Kopplin, P., Witt, M., Kaiser, K., et al. (2006). Characterization of a major refractory component of marine dissolved organic matter. *Geochim. Cosmochim. Acta* 70, 2990–3010. doi: 10.1016/j.gca.2006.03.021
- Hobbie, J. E., Daley, R. J., and Jasper, S. (1977). Use of Nuclepore filters for counting bacteria by fluorescence microscopy. *Appl. Environ. Microbiol.* 33, 1225–1228.
- Horai, H., Arita, M., Kanaya, S., Nihei, Y., Ikeda, T., Suwa, K., et al. (2010). MassBank: a public repository for sharing mass spectral data for life sciences. *J. Mass Spectrom.* 45, 703–714. doi: 10.1002/jms.1777
- Jiao, N., Herndl, G. J., Hansell, D. A., Benner, R., Kattner, G., Wilhelm, S. W., et al. (2010). Microbial production of recalcitrant dissolved organic matter: long-term carbon storage in the global ocean. *Nat. Rev. Microbiol.* 8, 593–599. doi: 10.1038/nrmicro2386
- Jumars, P. A., Penry, D. L., Baross, J. A., Perry, M. J., and Frost, B. W. (1989). Closing the microbial loop: dissolved carbon pathway to heterotrophic bacteria from incomplete ingestion, digestion and absorption in animals. *Deep Sea Res.* 36, 483–495. doi: 10.1016/0198-0149(89)90001-0
- Jürgens, K., and Massana, R. (2008). “Protistan grazing on marine bacterioplankton,” in *Microbial Ecology of the Oceans*, ed D. L. Kirchman (New York, NY: Wiley), 383–441.
- Kaiser, K., and Benner, R. (2008). Major bacterial contribution to the ocean reservoir of detrital organic carbon and nitrogen. *Limnol. Oceanogr.* 53, 99–112. doi: 10.4319/lo.2008.53.1.0099
- Kawasaki, N., and Benner, R. (2006). Bacterial release of dissolved organic matter during cell growth and decline: Molecular origin and composition. *Limnol. Oceanogr.* 51, 2170–2180. doi: 10.4319/lo.2006.51.5.2170
- Kido Soule, M. C., Longnecker, K., Giovannoni, S. J., and Kujawinski, E. B. (2010). Impact of instrument and experimental parameters on the repeatability and reproducibility of peaks in ultrahigh resolution ESI FT-ICR mass spectra of natural organic matter. *Org. Geochem.* 41, 725–733. doi: 10.1016/j.orggeochem.2010.05.017
- Kido Soule, M. C., Longnecker, K., Johnson, W. M., and Kujawinski, E. B. (2015). Environmental metabolomics: analytical strategies. *Mar. Chem.* 177, 374–387. doi: 10.1016/j.marchem.2015.06.029
- Koch, B. P., Dittmar, T., Witt, M., and Kattner, G. (2007). Fundamentals of molecular formula assignment to ultrahigh resolution mass data of natural organic matter. *Anal. Chem.* 79, 1758–1763. doi: 10.1021/ac061949s
- Kujawinski, E. B. (2011). The impact of microbial metabolism on marine dissolved organic matter. *Ann. Rev. Mar. Sci.* 3, 567–599. doi: 10.1146/annurev-marine-120308-081003
- Kujawinski, E. B., and Behn, M. D. (2006). Automated analysis of electrospray ionization Fourier transform ion cyclotron resonance mass spectra of natural organic matter. *Anal. Chem.* 78, 4363–4373. doi: 10.1021/ac0600306
- Kujawinski, E. B., Del Vecchio, R., Blough, N. V., Klein, G. C., and Marshall, A. G. (2004). Probing molecular-level transformations of dissolved organic matter: insights from electrospray ionization Fourier-transform ion cyclotron resonance mass spectrometry. *Mar. Chem.* 92, 23–37. doi: 10.1016/j.marchem.2004.06.038
- Kujawinski, E. B., Longnecker, K., Blough, N. V., Del Vecchio, R., Finlay, L., Kitner, J. B., et al. (2009). Identification of possible source markers in marine dissolved organic matter using ultrahigh resolution electrospray ionization Fourier-transform ion cyclotron resonance mass spectrometry. *Geochim. Cosmochim. Acta* 73, 4384–4399. doi: 10.1016/j.gca.2009.04.033
- Lechtenfeld, O. J., Hertkorn, N., Shen, Y., Witt, M., and Benner, R. (2015). Marine sequestration of carbon in bacterial metabolites. *Nat. Commun.* 6, 6711. doi: 10.1038/ncomms7711
- Lima-Mendez, G., Faust, K., Henry, N., Decelle, J., Colin, S., Carcillo, F., et al. (2015). Determinants of community structure in the global plankton interactome. *Science* 348, 1262073. doi: 10.1126/science.1262073
- Longnecker, K., Da Costa, A., Bhatia, M., and Kujawinski, E. B. (2009). Effect of carbon addition and predation on acetate-assimilating bacterial cells in groundwater. *FEMS Microbiol. Ecol.* 70, 456–470. doi: 10.1111/j.1574-6941.2009.00767.x
- Longnecker, K., Futrelle, J., Coburn, E., Kido Soule, M. C., and Kujawinski, E. B. (2015a). Environmental metabolomics: databases and tools for data analysis. *Mar. Chem.* 177, 366–373. doi: 10.1016/j.marchem.2015.06.012
- Longnecker, K., Kido Soule, M. C., and Kujawinski, E. B. (2015b). Dissolved organic matter produced by *Thalassiosira pseudonana*. *Mar. Chem.* 168, 114–123. doi: 10.1016/j.marchem.2014.11.003
- Mantini, D., Petrucci, F., Pieragostino, D., Del Boccio, P., Di Nicola, M., Di Ilio, C., et al. (2007). LIMPIC: a computational method for the separation of protein MALDI-TOF-MS signals from noise. *BMC Bioinformatics* 8:101. doi: 10.1186/1471-2105-8-101
- Matz, C., and Jürgens, K. (2003). Interaction of nutrient limitation and protozoan grazing determines the phenotypic structure of a bacterial community. *Microb. Ecol.* 45, 384–398. doi: 10.1007/s00248-003-2000-0
- McCune, B., and Grace, J. (2002). *Analysis of Ecological Communities*. Glenden Beach, OR: MjM Software Design.
- Mou, X. Z., Sun, S. L., Edwards, R. A., Hodson, R. E., and Moran, M. A. (2008). Bacterial carbon processing by generalist species in the coastal ocean. *Nature* 451, 708–U704. doi: 10.1038/nature06513
- Nagata, T. (2000). “Production mechanisms of dissolved organic matter,” in *Microbial Ecology of the Oceans, 1st Edn.*, ed D. L. Kirchman (New York, NY: Wiley-Liss, Inc.), 121–152.

- Nagata, T., and Kirchman, D. L. (1991). Release of dissolved free and combined amino acids by bacterivorous marine flagellates. *Limnol. Oceanogr.* 36, 433–443. doi: 10.4319/lo.1991.36.3.0433
- Nagata, T., and Kirchman, D. L. (1992). Release of macromolecular organic complexes by heterotrophic marine flagellates. *Mar. Ecol. Prog. Ser.* 83, 233–240. doi: 10.3354/meps083233
- Ogawa, H., Amagai, Y., Koike, I., Kaiser, K., and Benner, R. (2001). Production of refractory dissolved organic matter by bacteria. *Science* 292, 917–920. doi: 10.1126/science.1057627
- Osterholz, H., Niggemann, J., Giebel, H. A., Simon, M., and Dittmar, T. (2015). Inefficient microbial production of refractory dissolved organic matter in the ocean. *Nat. Commun.* 6, 7422. doi: 10.1038/ncomms8422
- Passow, U. (2002). Production of transparent exopolymer particles (TEP) by phyto- and bacterioplankton. *Mar. Ecol. Prog. Ser.* 236, 1–12. doi: 10.3354/meps236001
- Paul, C., Barofsky, A., Vidoudez, C., and Pohnert, G. (2009). Diatom exudates influence metabolism and cell growth of co-cultured diatom species. *Mar. Ecol. Prog. Ser.* 389, 61–79. doi: 10.3354/meps08162
- Pedler Sherwood, B., Shaffer, E. A., Reyes, K., Longnecker, K., Aluwihare, L. I., and Azam, F. (2015). Metabolic characterization of a model heterotrophic bacterium capable of significant chemical alteration of marine dissolved organic matter. *Mar. Chem.* 177, 357–365. doi: 10.1016/j.marchem.2015.06.027
- Pernthaler, J. (2005). Predation on prokaryotes in the water column and its ecological implications. *Nat. Rev. Microbiol.* 3, 537–546. doi: 10.1038/nrmicro1180
- Rasche, F., Svatoš, A., Maddula, R. K., Böttcher, C., and Böcker, S. (2011). Computing fragmentation trees from tandem mass spectrometry data. *Anal. Chem.* 83, 1243–1251. doi: 10.1021/ac101825k
- Santoro, A. E., and Casciotti, K. L. (2011). Enrichment and characterization of ammonia-oxidizing archaea from the open ocean: phylogeny, physiology and stable isotope fractionation. *ISME J.* 5, 1796–1808. doi: 10.1038/ismej.2011.58
- Sarmento, H., Romera-Castillo, C., Lindh, M., Pinhassi, J., Sala, M. M., Gasol, J. M., et al. (2013). Phytoplankton species-specific release of dissolved free amino acids and their selective consumption by bacteria. *Limnol. Oceanogr.* 58, 1123–1135. doi: 10.4319/lo.2013.58.3.1123
- Schleifer, K.-H., and Kandler, O. (1972). Peptidoglycan types of bacterial cell walls and their taxonomic implications. *Bacteriol. Rev.* 36, 407–477.
- Sher, D., Thompson, J. W., Kashtan, N., Croal, L., and Chisholm, S. W. (2011). Response of *Prochlorococcus* ecotypes to co-culture with diverse marine bacteria. *ISME J.* 5, 1125–1132. doi: 10.1038/ismej.2011.1
- Sherr, E. B., and Sherr, B. F. (1994). Bacterivory and herbivory: key roles of phagotrophic protists in pelagic food webs. *Microb. Ecol.* 28, 223–235. doi: 10.1007/BF00166812
- Sleighter, R. L., and Hatcher, P. G. (2008). Molecular characterization of dissolved organic matter (DOM) along a river to ocean transect of the lower Chesapeake Bay by ultrahigh resolution electrospray ionization Fourier transform ion cyclotron resonance mass spectrometry. *Mar. Chem.* 110, 140–152. doi: 10.1016/j.marchem.2008.04.008
- Southam, A. D., Payne, T. G., Cooper, H. J., Arvanitis, T. N., and Viant, M. R. (2007). Dynamic range and mass accuracy of wide-scan direct infusion nano-electrospray Fourier transform ion cyclotron resonance mass spectrometry-based metabolomics increased by the spectral stitching method. *Anal. Chem.* 79, 4595–4602. doi: 10.1021/ac062446p
- Steinberg, D. K., Nelson, N. B., Carlson, C. A., and Prusak, A. C. (2004). Production of chromophoric dissolved organic matter (CDOM) in the open ocean by zooplankton and the colonial cyanobacterium *Trichodesmium*. *Mar. Ecol. Prog. Ser.* 267, 45–56. doi: 10.3354/meps267045
- Stodereger, K., and Herndl, G. J. (1998). Production and release of bacterial capsular material and its subsequent utilization by marine bacterioplankton. *Limnol. Oceanogr.* 43, 877–884. doi: 10.4319/lo.1998.43.5.0877
- Strom, S. L., Benner, R., Ziegler, S., and Dagg, M. J. (1997). Planktonic grazers are a potentially important source of marine dissolved organic carbon. *Limnol. Oceanogr.* 42, 1364–1374. doi: 10.4319/lo.1997.42.6.1364
- Tautenhahn, R., Cho, K., Uritboonthai, W., Zhu, Z., Patti, G. J., and Siuzdak, G. (2012). An accelerated workflow for untargeted metabolomics using the METLIN database. *Nat. Biotechnol.* 30, 826–828. doi: 10.1038/nbt.2348
- Taylor, G., Iturriaga, R., and Sullivan, C. W. (1985). Interactions of bacterivorous grazers and heterotrophic bacteria with dissolved organic matter. *Mar. Ecol. Prog. Ser.* 23, 129–141. doi: 10.3354/meps023129
- Wang, H., Jiang, L., and Weitz, J. S. (2009). Bacterivorous grazers facilitate organic matter decomposition: a stoichiometric modeling approach. *FEMS Microbiol. Ecol.* 69, 170–179. doi: 10.1111/j.1574-6941.2009.00699.x
- Watrous, J., Roach, P., Alexandrov, T., Heath, B. S., Yang, J. Y., Kersten, R. D., et al. (2012). Mass spectral molecular networking of living microbial colonies. *Proc. Natl. Acad. Sci. U.S.A.* 109, E1743–E1752. doi: 10.1073/pnas.1203689109
- Weber, R. J. M., Selander, E., Sommer, U., and Viant, M. R. (2013). A stable-isotope mass spectrometry-based metabolic footprinting approach to analyze exudates from phytoplankton. *Mar. Drugs* 11, 4158–4175. doi: 10.3390/md11114158
- Williams, D. K., and Muddiman, D. C. (2007). Parts-per-billion mass measurement accuracy achieved through the combination of multiple linear regression and automatic gain control in a Fourier transform ion cyclotron resonance mass spectrometer. *Anal. Chem.* 79, 5058–5063. doi: 10.1021/ac0704210
- Wu, D., Hartman, A., Ward, N., and Eisen, J. A. (2008). An automated phylogenetic tree-based small subunit rRNA taxonomy and alignment pipeline (STAP). *PLoS ONE* 3:e2566. doi: 10.1371/annotation/c1aa8dd-4360-4902-8599-4d7edca79817

Conflict of Interest Statement: The authors declare that the research was conducted in the absence of any commercial or financial relationships that could be construed as a potential conflict of interest.

Copyright © 2016 Kujawinski, Longnecker, Barott, Weber and Kido Soule. This is an open-access article distributed under the terms of the Creative Commons Attribution License (CC BY). The use, distribution or reproduction in other forums is permitted, provided the original author(s) or licensor are credited and that the original publication in this journal is cited, in accordance with accepted academic practice. No use, distribution or reproduction is permitted which does not comply with these terms.